# Spiro-Linked Ter-, Penta-, and Heptafluorenes as Novel Amorphous Materials for Blue Light Emission

D. Katsis,[†] Y. H. Geng,[†] J. J. Ou,[†] S. W. Culligan,[†] A. Trajkovska,[†] Shaw H. Chen,*[,†,‡] and L. J. Rothberg[†,§]

*Departments of Chemical Engineering and Chemistry, and Laboratory for Laser Energetics, Center for Optoelectronics and Imaging, University of Rochester, 240 East River Road, Rochester, New York 14623-1212*

*Received September 21, 2001. Revised Manuscript Received January 2, 2002*

A series of spiro-linked oligofluorenes were synthesized that exhibit blue emission with photoluminescence quantum yields in some cases exceeding 0.50 in neat spin-coated films. Differential scanning calorimetry revealed highly variable glass transition temperatures. A longer conjugation length is desired for better stability against thermally activated crystallization, and a shorter pendant is desired for a higher glass transition temperature at a given conjugation length. In contrast to poly(2,7-(9,9-di-*n*-octylfluorene)), prolonged heating of spiro-oligo(fluorene) films resulted in no changes in morphology, emissive color, and photoluminescence quantum yield. The propensity of spiro-oligo(fluorene)s to thermally activated crystallization was rationalized with molecular shapes predicted by molecular mechanics simulations.

## Introduction

Organic electroluminescent displays have gained tremendous momentum toward a mature technology because of simple systems design, wide viewing angles, and potentially low power consumption compared to liquid crystal displays. Two distinct material approaches have been pursued: low molecular weight substances that can be vacuum-deposited[1] and conjugated polymers that can be spin-coated.[2] Blue emission has remained a materials challenge to full-color display in terms of quantum efficiency and color stability, for which poly(fluorene)s have emerged as the prime conjugated polymer candidates.[3−10] In particular, amorphous materials with an elevated glass transition temperature, $T_g$, and with structural features that prevent $\pi$-stacking are desired. However, both polymer structure and film processing conditions have been found to affect interchain interactions and nanoscale morphology that are critical to emission characteristics.[11,12] To better control these structural features, conjugated oligomers with well-defined chain lengths and end groups appear to be particularly promising.[13] Conjugated oligomers are characterized by structural uniformity, absence of chain defects, and ease of purification, characterization, and processing into thin films. In comparison to polymers, oligomers generally possess more predictable and reproducible properties that are amenable to optimization through molecular engineering. Nonetheless, it is highly desirable to endow oligomers with a high $T_g$ and superior morphological stability against crystallization. Therefore, glass-forming amorphous[14−19] and mesomorphic[20−22] molecular materials have been sought after for electronic, optical, photonic, and optoelectronic applications. In particular, spiro-linked oligo(*p*-phenylene)s stand out in their ability to form varied amorphous

* To whom correspondence should be addressed.
[†] Department of Chemical Engineering.
[‡] Laboratory for Laser Energetics.
[§] Department of Chemistry.

(1) Tang, C. W.; VanSlyke, S. A. *Appl. Phys. Lett.* **1987**, *51*, 913.
(2) Burroughes, J. H.; Bradley, D. D. C.; Brown, A. R.; Marks, R. N.; Mackay, K.; Friend, R. H.; Burn, P. L.; Holmes, A. B. *Nature* **1990**, *347*, 539.
(3) Bliznyuk, V. N.; Carter, S. A.; Scott, J. C.; Klärner, G.; Miller, R. D.; Miller, D. C. *Macromolecules* **1999**, *32*, 361.
(4) Leclerc, M. *J. Polym. Sci., Part A: Polym. Chem.* **2001**, *39*, 2867.
(5) Klärner, G.; Lee, J.-K.; Davey, M. H.; Miller, R. D. *Adv. Mater.* **1999**, *11*, 115.
(6) Klärner, G.; Lee, J.-I.; Chan, F.; Chen, J.-P.; Nelson, A.; Markiewicz, D.; Siemens, R.; Scott, J. C.; Miller, R. D. *Chem. Mater.* **1999**, *11*, 1800.
(7) Yu, W.-L.; Pei, J.; Huang, W.; Heeger, A. J. *Adv. Mater.* **2000**, *12*, 828.
(8) Sainova, D.; Miteva, T.; Nothofer, H. G.; Scherf, U.; Glowaki, I.; Ulanski, J.; Fujikawa, H.; Neher, D. *Appl. Phys. Lett.* **2000**, *76*, 1810.
(9) Setayesh, S.; Grimsdale, A. C.; Weil, T.; Enkelmann, V.; Müllen, K.; Meghdadi, F.; List, E. J. W.; Leising, G. *J. Am. Chem. Soc.* **2001**, *123*, 946.
(10) Marsitzky, D.; Vestberg, R.; Blainey, P.; Tang, B. T.; Hawker, C. J.; Carter, K. R. *J. Am. Chem. Soc.* **2001**, *123*, 6965.
(11) Nguyen, T.-Q.; Martini, I. B.; Liu, J.; Schwartz, B. J. *J. Phys. Chem. B* **2000**, *104*, 237.
(12) Teetsov, J. A.; Vandan Bout, D. A. *J. Phys. Chem. B* **2000**, *104*, 9378; *J. Am. Chem. Soc.* **2001**, *123*, 3605.
(13) Müllen, K.; Wegner, G. *Electronic Materials: The Oligomer Approach*; Wiley-VCH: Weinheim, New York, 1998.
(14) Katsuma, K.; Shirota, Y. *Adv. Mater.* **1998**, *10*, 223.
(15) Steuber, F.; Staudigel, J.; Stössel, M.; Simmerer, J.; Winnacker, A.; Spreitzer, H.; Weissörtel, F.; Salbeck, J. *Adv. Mater.* **2000**, *12*, 130.
(16) Bach, U.; De Cloedt, K.; Spreitzer, H.; Grätzel, M. *Adv. Mater.* **2000**, *12*, 1060.
(17) Robinson, M. R.; Wang, S.; Bazan, G. C.; Cao, Y. *Adv. Mater.* **2000**, *12*, 1701.
(18) O'Brien, D. F.; Burrows, P. F.; Forrest, S. R.; Koene, B. E.; Loy, D. E.; Thompson, M. E. *Adv. Mater.* **1998**, *10*, 1108.
(19) (a) Salbeck, J.; Yu, N.; Bauer, J.; Weissörtel; Bestgen, H. *Synth. Met.* **1997**, *91*, 209. (b) Johansson, N.; Salbeck, J.; Bauer, J.; Weissörtel, F.; Bröms, P.; Andersson, A.; Salaneck, W. R. *Adv. Mater.* **1998**, *10*, 1136.
(20) Chen, S. H.; Shi, H.; Conger, B. M.; Mastrangelo, J. C.; and Tsutsui, T. *Adv. Mater.* **1996**, *8*, 998
(21) Tamaoki, N. *Adv. Mater.* **2001**, *13*, 1135.
(22) Chen, H. P.; Katsis, D.; Mastrangelo, J. C.; Chen, S. H.; Jacobs, S. D.; Hood, P. J. *Adv. Mater.* **2000**, *12*, 1283.

10.1021/cm010679l CCC: $22.00 
Published on Web 02/09/2002

**Scheme 1. Synthesis of Spiro-oligo(fluorene)s 8a, 8b, 9a, 9b, and 10**[a]

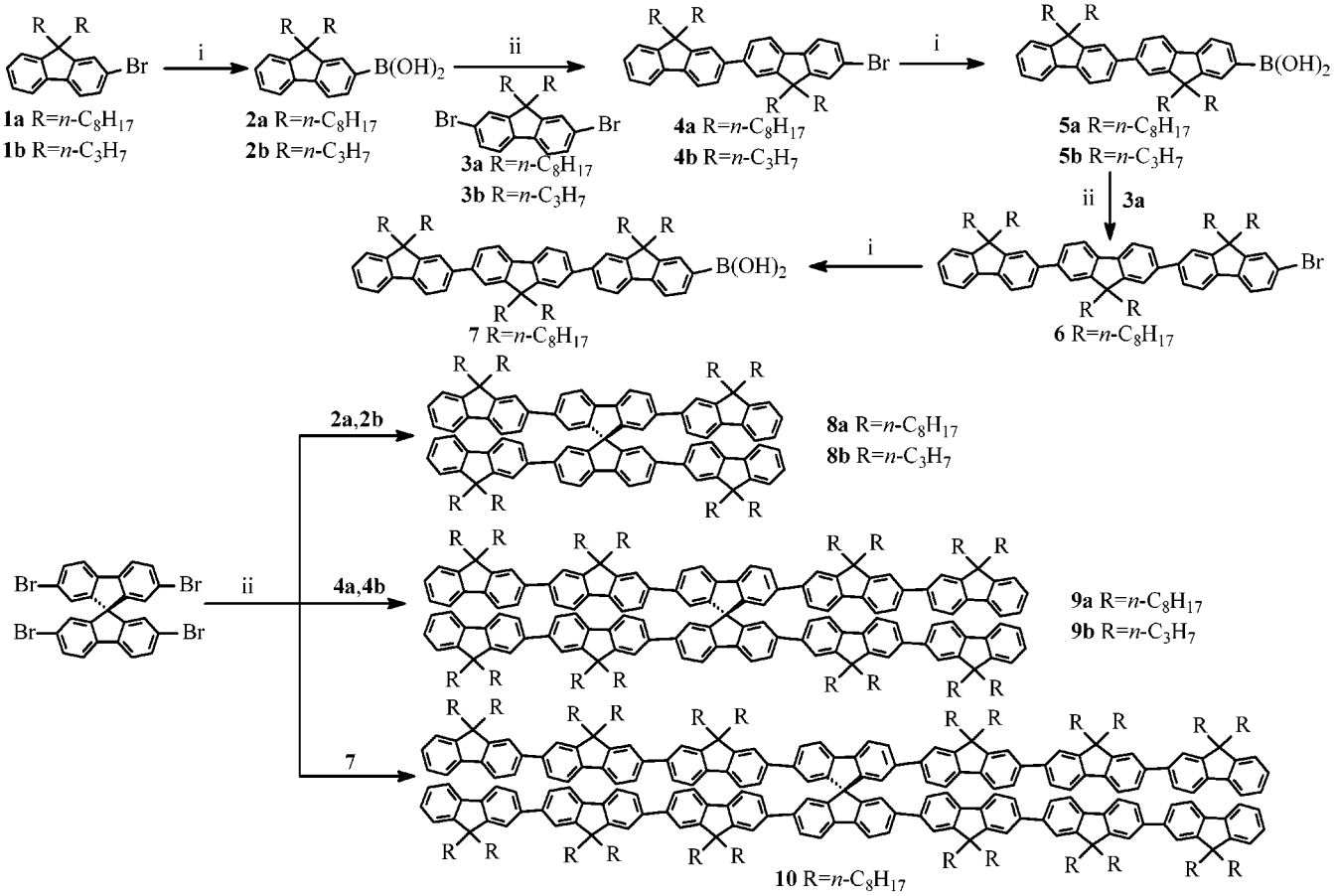


[a] 1. (i) *n*-BuLi, −78 °C, (ii) (*i*-PrO)$_3$B, −78 °C to RT, (iii) HCl (2 M); 2. Pd(PPh$_3$)$_4$, Na$_2$CO$_3$ (2.0 M *aq*.), toluene, 90 °C.

glasses.[15,16,19] In what follows, we report on the synthesis, characterization, and molecular simulation of a novel class of spiro-linked oligo(fluorene)s for stable and efficient blue emission.

## Results and Discussion

On the basis of Scheme 1, five spiro-linked oligo(fluorene)s carrying *n*-propyl and *n*-octyl pendants were synthesized with their molecular structures elucidated by elemental analysis and $^1$H NMR spectroscopy. As an illustration, the $^1$H NMR spectra of **8b** and **9b** are presented in Figure 1. Signals were assigned based on reported chemical shifts,[23−25] coupling constants, and the spectra collected for intermediates and precursors. Note the downfield shift of the **9b** spectrum from that of **8b** because of the greater extent of $\pi$-conjugation. With these target compounds, the effects of structural features on $T_g$ and stability against thermally activated crystallization were investigated.

Poly(fluorene)s are generally stable up to 400 °C without thermal decomposition.[5,9] Differential scanning calorimetry (DSC) and polarizing optical microscopy were employed to determine phase transition temperatures. Compiled in Figure 2 are the DSC heating scans at 20 °C/min of samples that have been melted with subsequent cooling to −30 °C. That **8b** sustained heating without decomposition was evidenced by both $T_g$ and $T_m$ staying constant to within ±0.1 °C in three heating−cooling cycles between 0 and 370 °C. Spiro-linked terfluorenes, **8a** and **8b**, undergo glass transition at 60 and 179 °C, respectively. Upon heating beyond $T_g$, **8a** and **8b** were found to crystallize, respectively, at 84 and 243 °C, referred to as the crystallization temperature, $T_k$. This is an indication of morphological instability, as commonly encountered with nonpolymeric organic materials. Further heating revealed the crystalline melting point, $T_m$, at 194 and 348 °C for **8a** and **8b,** respectively. The enthalpies of phase transition are included to accompany the truncated peaks in Figure 2. In contrast, spiro-linked pentafluorenes, **9a** and **9b**, are morphologically stable upon heating beyond their respective $T_g$'s, 56 and 202 °C. Note that a shorter pendant contributes to an elevated $T_g$, **8b** vs **8a** and **9b** vs **9a**. The strong interaction between *n*-octyl pendants seems to predominate over the effect of conjugation length in view of **8a**, **9a**, and **10** all exhibiting a $T_g \sim$ 60 °C. With *n*-propyl pendants, an increase in conjugation length from three to five is accompanied by a 23 °C elevation in $T_g$.

(23) Fukuda, M.; Sawada, K.; Yoshino, K. *J. Polym. Sci., Part A: Polym. Chem*. **1993**, *31*, 2465.
(24) Ranger, M.; Leclerc, M. *Macromolecules* **1999**, *32*, 3306.
(25) Wu, R. L.; Schumm, J. S.; Pearson, D. L.; Tour, J. M. *J. Org. Chem*. **1996**, *61*, 6906.
(26) Jellison, G. E., Jr.; Modine, F. A. *Appl. Phys. Lett*. **1996**, *69*, 371 and 2137.
(27) Holzer, W.; Pichlmaier, M.; Drotleff, E.; Penzkofer, A.; Bradley, D. D. C.; Blau, W. J. *Opt. Commun*. **1999**, *163*, 24.

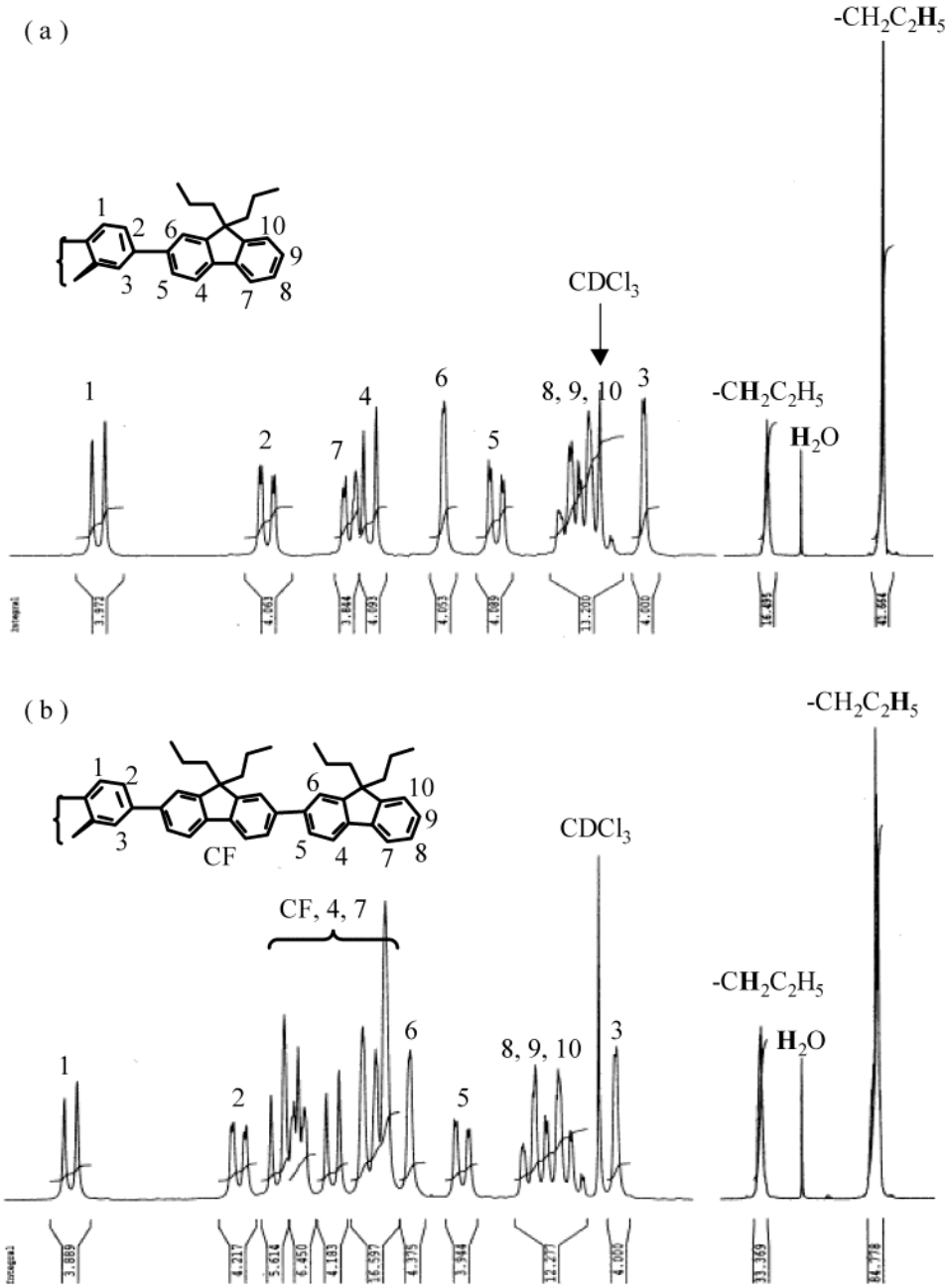


**Figure 1.** $^1$H NMR spectra (400 MHz, $CDCl_3$) of (a) **8b** and (b) **9b**.

The morphology of spin-coated films has a direct bearing on the feasibility of oligo(fluorene)s for device application. Since crystallization tends to create grain boundaries that limit charge transport and cause poor contact, glassy films with an elevated $T_g$ are desired for practical applications. Flakes of all five compounds were characterized to be amorphous by electron diffraction. The absorption and photoluminescence (PL) spectra of **8a**, **9a**, and **10** in dilute solutions and neat films on fused silica substrates are shown in Figure 3. Pristine films of **8a**, **9a**, and **10** show a 2−6 nm and 6−9 nm red-shift in absorption and PL, respectively, from dilute solutions, that are accountable with changes in dielectric environment or molecular conformation. Since photo-oxidation is a complicating factor in the photophysics of organic luminescent materials, oxygen and ambient light were excluded from thermal annealing. The intent was to address PL spectral instability as a result of nanoscale structural evolution. Thus, thermal annealing experiments were conducted at 70 °C (i.e., 10 °C above $T_g$) in argon for 96 h. The results shown in Figures 3c and 3d indicate very small changes in absorption and PL spectra and quantum yields, $\Phi_{PL}$, 0.44 ± 0.02 and 0.54 ± 0.02 for **9a** and **10**, respectively. In contrast, thermal treatment of the **8a** film led to a blue-shifted absorption spectrum with a reduced absorbance and a loss of vibronic structures in the PL spectrum, suggesting that molecules adopt a more twisted structure. Nevertheless, these minor changes did not compromise the desired stable blue emission. The fact that the quantum yield remains high, $\Phi_{PL} = 0.57 \pm 0.01$, is consistent with the intramolecular origin of the observed changes induced by thermal annealing. In all cases, the amorphous character of spin-coated films was found to persist upon prolonged heating as determined by electron diffraction. The observed $\Phi_{PL}$ values compare

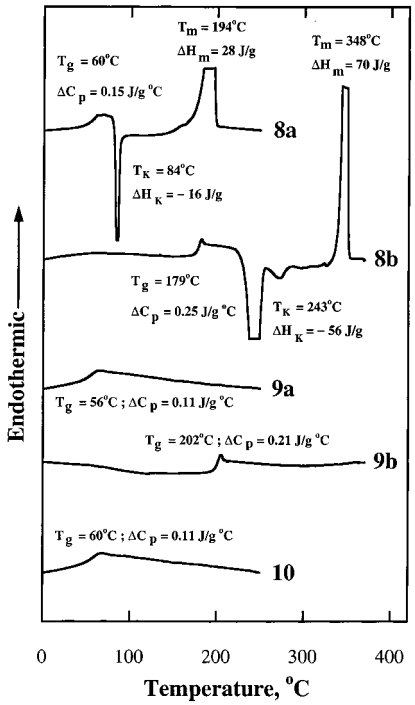


**Figure 2.** Heating scans at 20 °C/min of samples of spiro-oligofluorenes that have been preheated to isotropic liquids followed by cooling at −20 °C/min to −30 °C.

favorably with those of poly(fluorene)s structurally optimized to elevate $T_g$ and to prevent interchromophoric interactions.[7,10,29] Heating pristine films in air under otherwise identical conditions led to little loss in the PL intensity from the **8a** film but substantial losses from the **9a** and **10** films while retaining their amorphous character (see Supporting Information).

Within experimental uncertainties, the absorption and PL spectra in dilute solutions are not affected by the pendant's chain length, *n*-propyl in **8b** and **9b** (Figure 4a) vs *n*-octyl in **8a** and **9a** (Figure 3a), suggesting a constant torsion angle between neighboring fluorene units within the conjugated segments. In comparison to dilute solutions, pristine films' absorption spectra show no more than a 4 nm blue-shift while their PL spectra show a 5−10 nm red-shift; see Figures 4b and 4c. Stability tests of the **8b** and **9b** films were conducted in argon at 100 °C for 96 h. The amorphous character was found to persist, and both absorption and PL spectra remain largely intact. However, the *n*-propyl pendant seems to be responsible for 30 to 40% lower PL quantum yields than the *n*-octyl pendant, presumably because the *n*-octyl pendant is more effective in suppressing $\pi$-stacking. As a comparison, a 170 nm thick poly(2,7-(9,9-di-*n*-octylfluorene)), PF8, film was prepared for a stability test under the same conditions as **8b** and **9b**. Since PF8 is known to exhibit liquid crystalline mesomorphism upon heating beyond 170 °C,[31] precautions were taken to ensure that this film remained amorphous throughout the experimentation. As shown in Figure 4d, thermal treatment of an amorphous PF8 film resulted in spectral shift and excimer formation, causing undesirable emissive color instability.

To furnish insight into how molecular structure affects the observed properties in dilute solution and neat film, molecular mechanics simulation was performed on single molecules using the AMBER software package. The energy to be minimized accounts for all the interactions between bonded and nonbonded atoms in a given molecule. The spirobifluorene core and the 9,9-di-*n*-alkylfluorenyl unit were separately computed for the construction of **8a**, **8b, 9a**, and **9b**, whose final structures, as shown in Figure 5, are largely independent of the initially imposed torsion angle between neighboring fluorene units. The top views indicate that the two spiro-linked fluorene units are oriented at 90° with respect to each other, consistent with the X-ray single-crystal analysis, 88°, reported for 9,9′-spirobifluorene.[32] Furthermore, the torsion angles of all compounds fall within 28 ± 1°, consistent with the experimental observations that the absorption and PL spectra in dilute solutions are independent of pendant groups. The presented top and side views combine to permit visualization of overall molecular shapes. Because of the longer conjugation length in **9a** and **9b**, the resultant "shallow bowls" seem to prevent thermally activated crystallization. In contrast, the "flat plates" assumed by **8a** and **8b** are responsible for crystallization from isotropic melts above $T_g$, as shown in Figure 2. These insights suggest that molecular packing calculations will be useful in designing spiro-oligo(fluorene)s that resist crystallization while retaining their intramolecular photophysical properties.

## Conclusions

Novel spiro-oligo(fluorene)s with *n*-propyl and *n*-octyl pendants, that are readily soluble and processable into thin films, have been synthesized and characterized as stable and efficient blue light emitters. Key observations are recapitulated as follows:

(1) The amorphous character of spin-coated films of all compounds was found to persist upon prolonged heating. Furthermore, amorphous glasses of spiro-pentafluorenes and heptafluorenes were found to resist thermally activated crystallization. A $T_g$ of 202 °C was achieved with spiro-pentafluorene carrying *n*-propyl pendants. However, spiro-terfluorenes with *n*-propyl and *n*-octyl pendants were found to crystallize upon heating beyond $T_g$.

(2) Pristine films of the spiro-oligo(fluorene)s exhibited almost identical spectroscopy to that in dilute solution and have PL quantum yields close to 0.50. Furthermore, prolonged heating of neat films in argon resulted in practically no changes in emissive color or quantum yield. In contrast, thermal treatment of a poly(2,7-(9,9-di-*n*-octylfluorene)) film caused substantial emissive color instability.

(3) Molecular mechanics simulation yielded a 90° orientation between the two spiro-linked fluorene units, consistent with the reported single-crystal X-ray analy-

(28) Wang, X. H.; Grell, M.; Lane, P. A.; Bradley, D. D. C. *Synth. Met.* **2001**, *119*, 535.
(29) Klärner, G.; Davey, M. H.; Chen, W.-D.; Scott, J. C.; Miller, R. D. *Adv. Mater.* **1998**, *10*, 993.
(30) Pope, M.; Swenberg, C. E. *Electronic Processes in Organic Crystals and Polymers*, 2nd ed.; Oxford University Press: New York, NY, 1999.
(31) Grell, M.; Bradley, D. D. C.; Inbasekaran, M.; Woo, E. P. *Adv. Mater.* **1997**, *9*, 798.
(32) Schenk, H. *Acta Crystallogr.* **1972**, *B28*, 625.

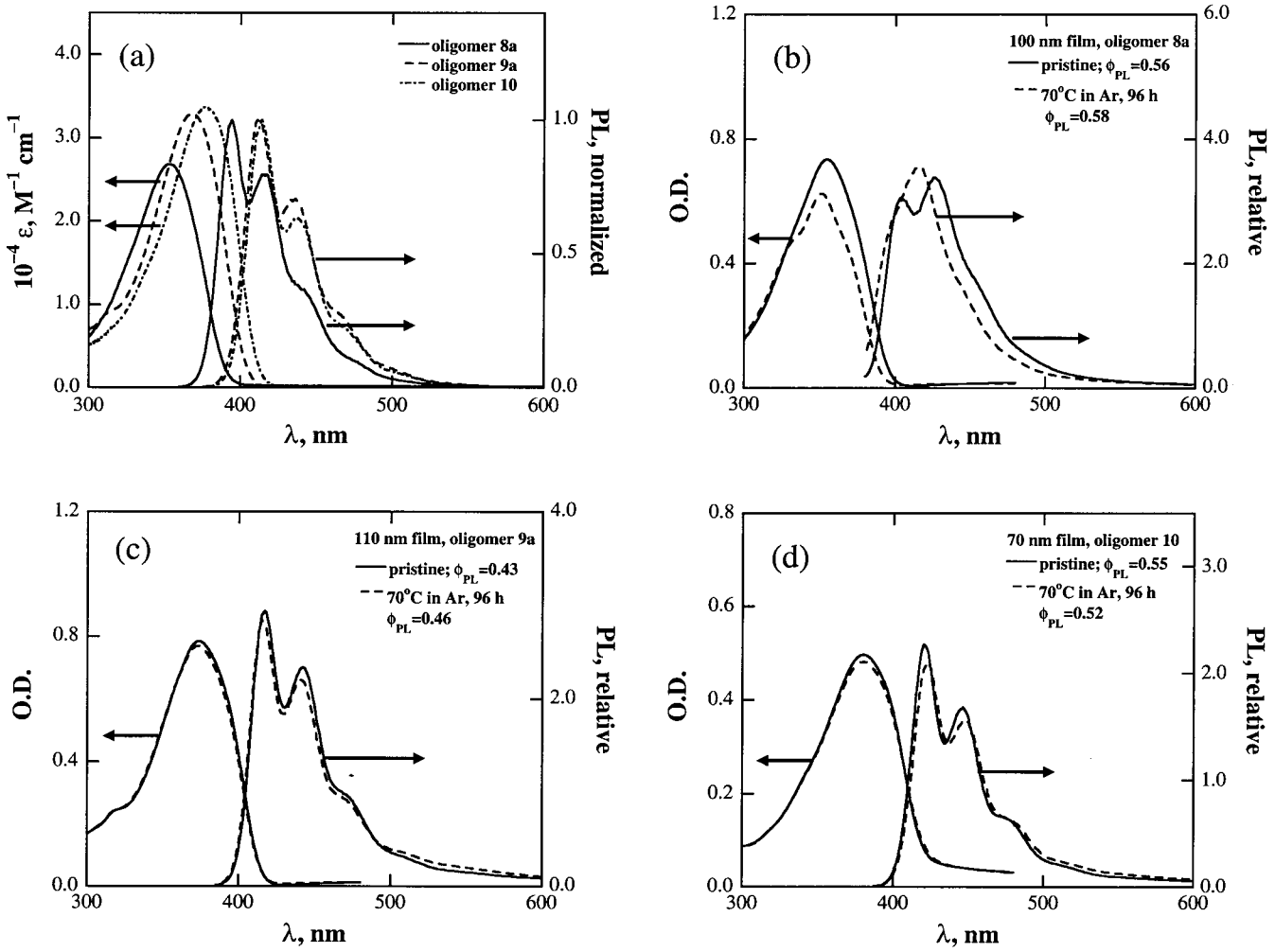


**Figure 3.** Absorption and photoluminescence (with excitation at 350 nm) spectra of (a) dilute solutions of **8a**, **9a**, and **10** in chloroform at $10^{-5}$ M based on fluorene monomer units, (b) neat film of **8a** before and after thermal treatment, (c) neat film of **9a** before and after thermal treatment, and (d) neat film of **10** before and after thermal treatment.

sis. The torsion angles between neighboring fluorene units within a conjugated segment were all evaluated at 28 ± 1°, consistent with the fact that the absorption and PL spectra in dilute solutions are independent of pendants. The molecular shapes revealed through molecular mechanics simulation are correlated with stability against thermally activated crystallization.

## Experimental Section

**Materials.** All chemicals, reagents, and solvents were used as received from commercial sources without further purification except tetrahydrofuran (THF) and toluene that had been distilled over sodium/benzophenone and sodium, respectively. Intermediates **1**, **3** and tetrabromo-9,9′-spirobifluorene were synthesized according to literature procedures.[25,33] Poly(2,7-(9,9-di-*n*-octylfluorene)) was prepared following literature procedures.[33] Anal. Calcd for $(C_{29}H_{40})_n$: C, 89.63; H, 10.37. Found: C, 89.68; H, 10.28. With the use of a size exclusion chromatograph equipped with serially arranged UV−vis absorbance detector, 15 and 90° light scattering detector, differential viscometer, and differential refractometer, as described previously,[34] the weight-average molecular weight was evaluated at 75 700 g/mole with a polydispersity index of 1.88.

**9,9-Di-*n*-octylfluorenyl-2-boronic acid (2a).** To a solution of 2-bromo-9,9-di-*n*-octylfluorene (12.0 g, 25.6 mmol) in anhydrous THF (50 mL) was slowly added *n*-BuLi (2.5 M in hexane, 12.0 mL, 30.0 mmol) at −78 °C. At this temperature, the reaction mixture was stirred for 1 h before adding tri-*iso*-propyl borate (9.0 mL, 7.34 g, 39.0 mmol). It was then warmed to room temperature, stirred overnight followed by quenching with 100 mL HCl (2.0 M), and poured into a large amount of water. After extraction with ethyl ether three times, the organic portions were washed with brine before drying over anhydrous $MgSO_4$. Solid residues collected by evaporating off the solvent were purified by column chromatography on silica gel with petroleum ether/ethyl acetate (2:1) to afford **2a** as white solids (10.0 g, 89%). $^1$H NMR (400 MHz, $CDCl_3$): $\delta$ 7.70−8.35 (m, fluorenyl *H*, 4H), 7.34−7.44 (m, fluorenyl *H*, 3H), 1.90−2.15 (m, $-CH_2C_7H_{15}$, 4H), 1.00−1.30 (m, $-CH_2CH_2-(CH_2)_5CH_3$, 20H), 0.83 (m, $-CH_3$, 6H), 0.71 (broad, $-CH_2CH_2-C_6H_{13}$, 2H), 0.60 (broad, $-CH_2CH_2C_6H_{13}$, 2H).

**9,9-Di-*n*-propylfluorenyl-2-boronic acid (2b).** The procedure for **2a** was followed to prepare **2b** from **1b** (6.00 g, 18.2 mmol) as white solids (4.10 g, 76%). $^1$H NMR (400 MHz, $CDCl_3$): $\delta$ 7.83−8.35 (m, fluorenyl *H*, 4H), 7.34−7.47 (m, fluorenyl *H*, 3H), 1.90−2.20 (m, $-CH_2C_2H_5$, 4H), 0.60−0.90 (m, $-CH_2C_2H_5$, 10H).

**7-Bromo-9,9,9′,9′-tetra-*n*-octyl-2,2′-bifluorene (4a).** A mixture of **2a** (2.0 g, 4.60 mmol), 2,7-dibromo-9,9-di-*n*-octylfluorene (**3a**, 4.0 g, 7.32 mmol), $Pd(PPh_3)_4$ (50 mg, 0.043 mmol), $Na_2CO_3$ (2.0 M aqueous solution, 12.0 mL, 24.0 mmol), and toluene (20 mL) was stirred at 90 °C for 2 days. After it was cooled to room temperature, 200 mL of petroleum ether

(33) Grell, M.; Knoll, W.; Lupo, D.; Meisel, A.; Miteva, T.; Neher, D.; Nothofer, H.-G.; Scherf, U.; Yasuda, A. *Adv. Mater.* **1999**, *11*, 671.
(34) Chen, H. P.; Katsis, D.; Mastrangelo, J. C.; Marshall, K. L.; Chen, S. H.; Mourey, T. H. *Chem. Mater.* **2000**, *12*, 2275.

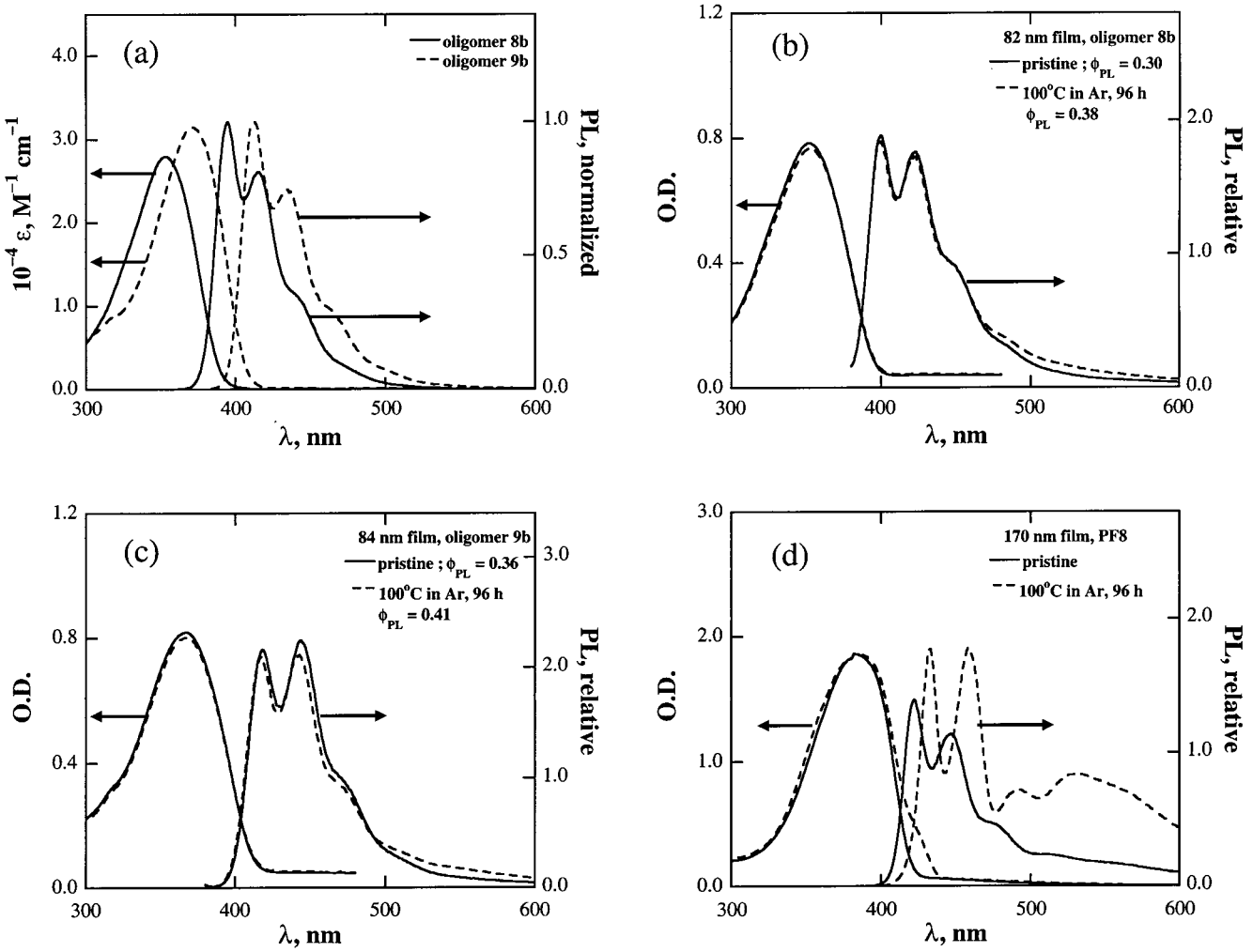


**Figure 4.** Absorption and photoluminescence (with excitation at 350 nm) spectra of (a) dilute solutions of **8b** and **9b** in chloroform at $10^{-5}$ M based on fluorene monomer units, (b) neat film of **8b** before and after thermal treatment, (c) neat film of **9b** before and after thermal treatment, and (d) neat film of PF8 before and after thermal treatment (PL spectra from excitation at 370 nm).

was added to the reaction mixture. The organic portion was separated and washed with brine before drying over anhydrous $MgSO_4$. The solvent was evaporated off, and the solid residues were purified by column chromatography on silica gel with petroleum ether to afford **4a** as white solids (2.52 g, 66%). $^1$H NMR (400 MHz, $CDCl_3$): $\delta$ 7.75 (d, $J$ = 7.84 Hz, fluorenyl $H$, 1H), 7.71 (d, $J$ = 7.72 Hz, fluorenyl $H$, 2H), 7.55−7.63 (m, fluorenyl $H$, 5H), 7.43−7.47 (m, fluorenyl $H$, 2H), 7.29−7.36 (m, fluorenyl $H$, 3H), 1.93−2.02 (m, $-CH_2C_7H_{15}$, 8H), 1.00−1.30 (m, $-CH_2CH_2(CH_2)_5CH_3$, 40H), 0.76−0.81 (m, $-CH_3$, 12H), 0.67 (broad, $-CH_2CH_2C_6H_{13}$, 8H).

**7-Bromo-9,9,9′,9′-tetra-*n*-propyl-2,2′-bifluorene (4b).** The procedure for **4a** was followed to prepare **4b** from **2b** (2.23 g, 7.58 mmol) and 2,7-dibromo-9,9-di-*n*-propylfluorene (**3b**, 10.0 g, 24.5 mmol) except for the use of petroleum ether/methylene chloride (95:5) for column chromatography to afford **4b** as white solids (3.18 g, 72%). $^1$H NMR (400 MHz, $CDCl_3$): $\delta$ 7.79 (d, $J$ = 7.82 Hz, fluorenyl $H$, 1H), 7.76 (d, $J$ = 7.84 Hz, fluorenyl $H$, 2H), 7.60−7.70 (m, fluorenyl $H$, 5H), 7.52 (d, $J$ = 1.45 Hz, fluorenyl $H$, 1H), 7.49 (dd, $J$ = 7.99 Hz, 1.75 Hz, fluorenyl $H$, 1H), 7.33−7.42 (m, fluorenyl $H$, 3H), 1.90−2.10 (broad, $-CH_2C_2H_5$, 8 H), 0.74 (broad, $-CH_2C_2H_5$, 20H).

**9,9,9′,9′-Tetra-*n*-octyl-2,2′-bifluorenyl-7-boronic acid (5a).** The procedure for **2a** was followed to prepare **5a** from **4a** (3.10 g, 3.61 mmol) as white solids (2.52 g, 85%). $^1$H NMR (400 MHz, $CDCl_3$): $\delta$ 7.92−8.41 (m, fluorenyl $H$, 3H), 7.63−7.85 (m fluorenyl $H$, 7H), 7.33−7.41 (m, fluorenyl $H$, 3H), 2.00−2.30 (m, $-CH_2C_7H_{15}$, 8H), 1.00−1.30 (m, $-CH_2CH_2(CH_2)_5CH_3$, 40H), 0.60−0.87 (m, $-CH_2CH_2C_6H_{13}$ and $-CH_3$, 20H).

**9,9,9′,9′-Tetra-*n*-propyl-2,2′-bifluorenyl-7-boronic acid (5b).** The procedure for **2a** was followed to prepare **5b** from **4b** (2.97 g, 5.14 mmol) as white solids (1.32 g, 47%). $^1$H NMR (400 MHz, $CDCl_3$): $\delta$ 7.92−8.41 (m, fluorenyl $H$, 3H), 7.64−7.85 (m, fluorenyl $H$, 7H), 7.34−7.44 (m, fluorenyl $H$, 3H), 2.00−2.30 (m, $-CH_2C_2H_5$, 8 H), 0.72−0.93 (m, $-CH_2C_2H_5$, 20H).

**7-Bromo-9,9,9′,9′,9″,9″-hexa-*n*-octyl-2, 7′;2′,7″-terfluorene (6).** The procedure for **4a** was followed to prepare **6** from **5a** (1.40 g, 1.70 mmol) and **3a** (1.86 g, 3.4 mmol) as white solids (1.25 g, 59%). $^1$H NMR (400 MHz, $CDCl_3$): $\delta$ 7.76−7.85 (m, fluorenyl H, 5H), 7.61−7.71 (m, fluorenyl $H$, 9H), 7.49−7.52 (m, fluorenyl $H$, 2H), 7.32−7.41 (m, fluorenyl $H$, 3H), 2.00−2.15 (m, $-CH_2C_7H_{15}$, 8H), 1.00−1.34 (m, $-CH_2CH_2(CH_2)_5CH_3$, 60H), 0.80−0.93 (m, $-CH_3$, 18H), 0.73 (broad, $-CH_2CH_2C_6H_{13}$, 12H).

**9,9,9′,9′,9″,9″-Hexa-*n*-octyl-2, 7′;2′,7″-terfluorenyl-7-boronic acid (7).** The procedure for **2a** was followed to prepare **7** (0.891 g, 79%) from **6** (1.16 g, 0.93 mol) as white solids. $^1$H NMR (400 MHz, $CDCl_3$): $\delta$ 7.85−8.42 (m, fluorenyl $H$, 2H), 7.7−7.83 (m, fluorenyl $H$, 14H), 7.36−7.4 (m, fluorenyl $H$, 3H), 2.00−2.24 (m, $-CH_2C_7H_{15}$, 8H), 1.00−1.30 (m, $-CH_2CH_2(CH_2)_5CH_3$, 60H), 0.79−0.86 (m, $-CH_3$, 18H), 0.75 (broad, $-CH_2CH_2C_6H_{13}$, 12H).

**General Procedure for the Preparation of 8, 9, and 10 via the Suzuki Coupling Reaction.** Toluene and a 2.0 M aqueous solution of $Na_2CO_3$ (60 equiv; toluene/water at a 6:4 ratio) were added to a Schlenk tube containing 2,2′,7,7′-tetrabromo-9,9′-spirobifluorene (1 equiv), boronic acids **2**, **5**, or **7** (6 equiv), and $Pd(PPh_3)_4$ (5 mol %). The reaction mixture

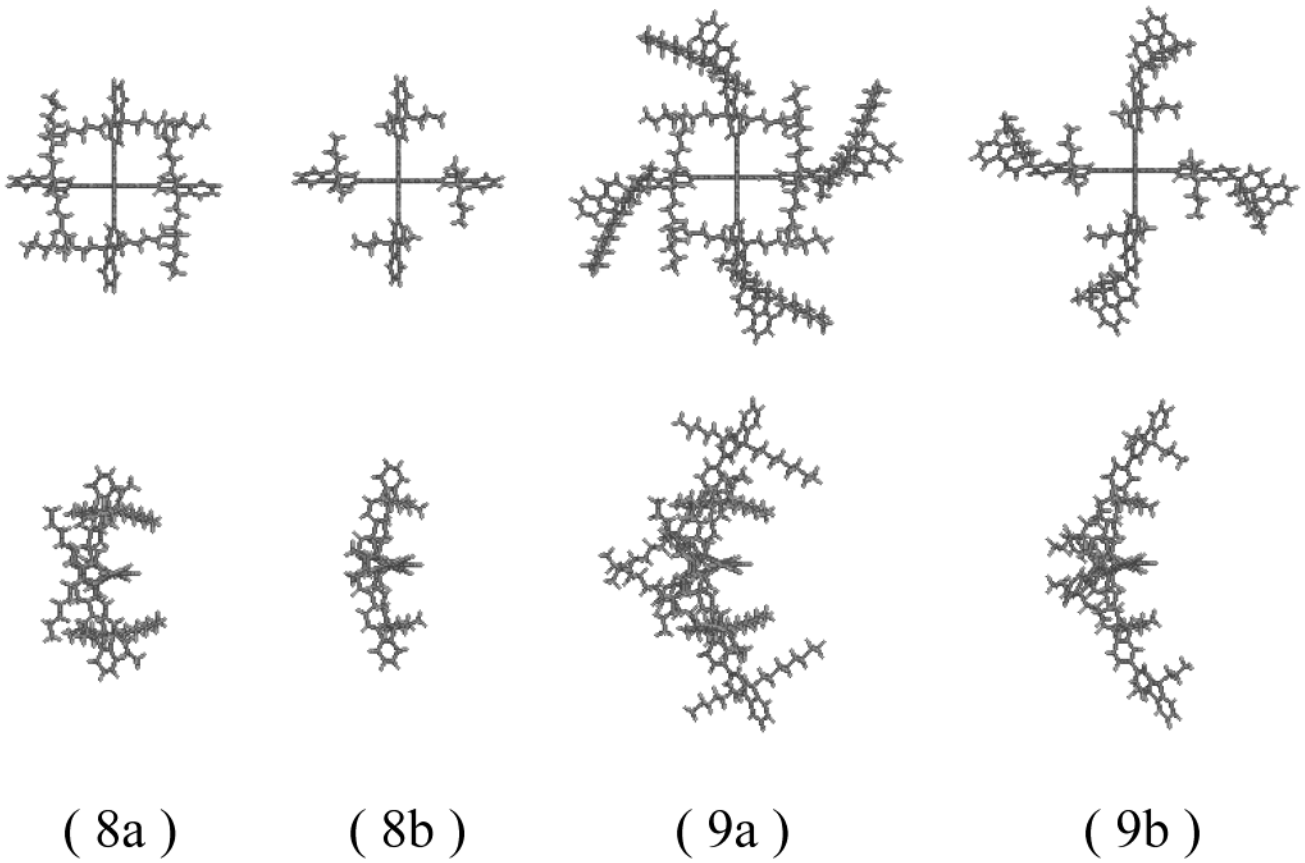


**Figure 5.** Top and side views of single molecules of **8a**, **8b**, **9a**, and **9b** from molecular mechanics simulation using the AMBER software package.

was stirred thoroughly at 90 °C for 2 days followed by the addition of a large amount of methylene chloride. The organic portion was washed with brine, dried over anhydrous $MgSO_4$, and concentrated by evaporating off the solvent for further purification by column chromatography on silica gel.

**2,2′,7,7′-Tetrakis(9,9-di-*n*-octylfluorenyl)-9,9′-spirobifluorene (8a).** The title compound was prepared from **2a** (1.00 g, 2.30 mmol) with column chromatography using petroleum ether/methylene chloride (8:1) as the eluent, resulting in a yield of 66% (0.49 g). $^1$H NMR (400 MHz, $CDCl_3$): $\delta$ 8.05 (d, $J$ = 7.96 Hz, spirobifluorenyl *H*, 4H), 7.78 (dd, $J$ = 7.97 Hz, 1.44 Hz, spirobifluorenyl *H*, 4H), 7.67 (dd, $J$ = 7.13 Hz, 1.31 Hz, fluorenyl *H*, 4H), 7.63 (d, $J$ = 7.92 Hz, fluorenyl *H*, 4H), 7.51 (d, $J$ = 1.05 Hz, fluorenyl *H*, 4H), 7.43 (dd, $J$ = 7.95 Hz, 1.39 Hz, fluorenyl *H*, 4H), 7.25−7.34 (m, fluorenyl *H*, 12H), 7.21 (d, $J$ = 1.03 Hz, spirobifluorenyl *H*, 4H), 1.96 (t, $J$ = 8.22 Hz, $-CH_2C_7H_{15}$, 16H), 1.00−1.30 (m, $CH_2CH_2(CH_2)_5CH_3$, 80H), 0.80 (t, $J$ = 7.11 Hz, $-CH_3$, 24H), 0.63 (broad, $-CH_2CH_2C_6H_{13}$, 16H). Anal. Calcd for $C_{141}H_{176}$: C, 90.52; H, 9.48. Found: C, 90.51; H, 9.38.

**2,2′,7,7′-Tetrakis(9,9-di-*n*-propylfluorenyl)-9,9′-spirobifluorene (8b).** The title compound was prepared from **2b** (1.80 g, 6.12 mmol) with column chromatography using petroleum ether/methylene chloride (4:1) as the eluent, resulting in a yield of 76% (1.00 g). $^1$H NMR (400 MHz, $CDCl_3$): $\delta$ 8.06 (d, $J$ = 7.97 Hz, spirobifluorenyl *H*, 4H), 7.79 (dd, $J$ = 7.96 Hz, 1.46 Hz, spirobifluorenyl *H*, 4H), 7.67 (dd, $J$ = 5.80 Hz, 1.58 Hz, fluorenyl *H*, 4H), 7.63 (d, $J$ = 7.91 Hz, fluorenyl *H*, 4H), 7.52 (d, $J$ = 0.92 Hz, fluorenyl *H*, 4H), 7.44 (dd, $J$ = 7.94 Hz, 1.39 Hz, fluorenyl *H*, 4H), 7.26−7.35 (m, fluorenyl *H*, 12H), 7.21 (d, $J$ = 1.28 Hz, spirobifluorenyl *H*, 4H), 1.95 (t, $J$ = 7.76 Hz, $-CH_2C_2H_5$, 16H), 0.62 (m, $-CH_2C_2H_5$, 40H). Anal. Calcd for $C_{101}H_{96}$: C, 92.61; H, 7.39. Found: C, 92.28; H, 7.50.

**2,2′,7,7′-Tetrakis(9,9,9′,9′-tetra-*n*-octyl-2,2′-bifluorenyl)-9, 9′-spirobifluorene (9a).** The title compound was prepared from **5a** (1.0 g, 1.21 mmol) with column chromatography using petroleum ether/methylene chloride (7:1) as the eluent, resulting in a yield of 50% (0.32 g). $^1$H NMR (400 MHz, $CDCl_3$): $\delta$ 8.09 (d, $J$ = 7.95 Hz, spirobifluorenyl *H*, 4H), 7.83 (dd, $J$ = 7.92 Hz, 1.02 Hz, spirobifluorenyl *H*, 4H), 7.74−7.80 (m, fluorenyl *H*, 12H), 7.69 (d, $J$ = 7.93 Hz, fluorenyl *H*, 4H), 7.56−7.65 (m, fluorenyl *H*, 20H), 7.49 (d, $J$ = 7.93 Hz, fluorenyl *H*, 4H), 7.30−7.39 (m, fluorenyl *H*, 12H), 7.26 (s, spirobifluorenyl *H*, 4H), 2.04 (broad, $-CH_2C_7H_{15}$, 32H), 1.00−1.34 (m, $-CH_2CH_2(CH_2)_5CH_3$, 160H), 0.66−0.84 (m, $-CH_3$, 48H), 0.64 (broad, $-CH_2CH_2C_6H_{13}$, 32H). Anal. Calcd for $C_{257}H_{336}$: C, 90.11; H, 9.89. Found: C, 89.59; H, 9.82.

**2,2′,7,7′-Tetrakis(9,9,9′,9′-tetra-*n*-propyl-2,2′-bifluorenyl)-9,9′-spirobifluorene (9b).** The title compound was prepared from **5b** (1.25 g, 2.30 mmol) with column chromatography using hexane/chloroform (2:1) as the eluent, resulting in a yield of 72% (0.66 g). $^1$H NMR (400 MHz, $CDCl_3$): $\delta$ 8.10 (d, $J$ = 7.96 Hz, spirobifluorenyl *H*, 4H), 7.84 (dd, $J$ = 8.02 Hz, 1.03 Hz, spirobifluorenyl *H*, 4H), 7.73−7.79 (m, fluorenyl *H*, 12 H), 7.69 (d, $J$ = 7.92 Hz, fluorenyl *H*, 4H), 7.57−7.65 (m, 20H), 7.49 (dd, $J$ = 7.95 Hz, 1.24 Hz, fluorenyl *H*, 4H), 7.30−7.41 (m, fluorenyl *H*, 12H), 7.26 (d, $J$ = 1.19 Hz, spirobifluorenyl *H*, 4H), 2.04 (broad, $-CH_2C_2H_5$, 32H), 0.66−0.75 (m, $CH_2C_2H_5$, 80H). Anal. Calcd for $C_{177}H_{176}$: C, 92.30; H, 7.70. Found: C, 92.05; H, 7.80.

**2,2′,7,7′-Tetrakis(9,9,9′,9′,9″,9″-hexa-*n*-octyl-2,7′;2′,7″-terfluorenyl)-9,9′-spirobifluorene (10).** The title compound was prepared from **5b** (0.800 g, 0.660 mmol) with column chromatography using petroleum ether/methylene chloride (6:1) as the eluent, resulting in a yield of 46% (0.25 g). $^1$H NMR (400 MHz, $CDCl_3$): $\delta$ 8.11 (d, $J$ = 7.94 Hz, spirobifluorenyl *H*, 4H), 7.76−7.86 (m, spirobifluorenyl and fluorenyl *H*, 24 H), 7.58−7.72 (m, fluorenyl *H*, 40H), 7.51 (d, $J$ = 8.27 Hz, fluorenyl *H*, 4 H), 7.32−7.41 (m, fluorenyl *H*, 12H), 7.24 (s, spirobifluorenyl *H*, 4H), 2.07 (broad, $-CH_2C_7H_{15}$, 48H), 1.00−1.30 (m, $-CH_2CH_2(CH_2)_5CH_3$, 240H), 0.60−0.90 (m, $-CH_3$ and $-CH_2CH_2C_6H_{13}$, 120H). Anal. Calcd for $C_{373}H_{496}$: C, 89.96; H, 10.04. Found: C, 89.86; H, 10.04.

**Molecular Structures, Morphology, and Thermal Transition Temperatures.** $^1$H NMR spectra were acquired in $CDCl_3$ with an Avance-400 spectrometer (400 MHz). Elemental analysis was carried out by Galbraith Laboratories, Inc. Thermal transition temperatures were determined by DSC (Perkin-Elmer DSC-7) with a continuous $N_2$ purge at 20 mL/min. Samples were preheated to isotropic liquids followed by cooling at −20 °C/min to −30 °C before taking the reported second heating scans at 20 °C/min. Morphology and the nature of phase transition were characterized with a polarizing optical microscope (DMLM, Leica, FP90 central processor and FP82 hot stage, Mettler Toledo).

**Film Preparation and Characterization.** Thin films on the order of 100 nm in thickness were prepared by spin-coating from 1.0 wt % solutions in chloroform at 5000 rpm on optically flat, fused silica substrates (25.4 mm diameter × 3 mm thickness; Esco products; transparent down to 200 nm) followed by vacuum-drying at room temperature overnight. A UV−vis−NIR spectrophotometer was used to measure absorption spectra in dilute solution and neat film. PL was characterized with a spectrofluorimeter (Quanta Master C-60SE, Photon Technology International). The dilute solution spectra were taken in a 90° arrangement between excitation and detection beams. In the case of solid films, a straight-through arrangement was adopted in which a liquid light guide (Photon Technology International) was used to direct an excitation beam at 350 nm onto the center of the film; the light guide also served as a polarization randomizer. Approximately 100 nm thick flakes for electron diffraction were prepared following the same procedures except on single-crystal NaCl substrates (International Crystal Laboratories) and then floated off in a trough filled with deionized water for mounting onto copper grids. Electron diffraction was performed on a transmission electron microscope (JEM 2000 EX, JEOL USA).

**Photoluminescence Quantum Yield.** As the primary standard for PL quantum yield ($\Phi_{PL}$), 9,10-diphenylanthracene (99%, Acros Organics) was repeatedly recrystallized from xylenes until pale yellow prism crystals were obtained. Anthracene (99%, Aldrich Chemical Co.) was recrystallized from ethanol. Poly(methyl methacrylate) (PMMA, Polysciences) with a weight-average molecular weight of 75 000 was used without further purification. About 5 $\mu$m thick PMMA films doped with 9,10-diphenylanthracene and anthracene at $10^{-2}$ M were spin-cast on fused silica substrates followed by drying in vacuo overnight. A low doping level was adopted to avoid concentration quenching, entailing the much thicker film than neat films of spiro-oligo(fluorene)s. The film lightly doped with 9,10-diphenylanthracene was assigned a widely accepted value, $\Phi_{PL} = 0.83$.[35] The anthracene-containing film was characterized with the following formula[36]

$$\frac{\Phi_{PL,s}}{\Phi_{PL,r}} = \frac{1 - 10^{-A_r}}{1 - 10^{-A_s}} \frac{B_s \overline{n_s^2}}{B_r \overline{n_r^2}} \quad (1)$$

where subscripts s and r refer to sample and reference, respectively, $A$ denotes absorbance at the excitation wavelength, $B$ is the integrated intensity across the entire emission spectrum, and $\overline{n^2}$ is defined as follows

$$\overline{n^2} \equiv \frac{\int I(\lambda) n^2(\lambda)\, d\lambda}{\int I(\lambda)\, d\lambda} \quad (2)$$

in which $I(\lambda)$ stands for emission intensity, and the integration is performed over the entire emission spectrum. A variable angle spectroscopic ellipsometer (V-VASE, J. A. Woollam) was employed to collect data at four incident angles (55, 60, 62, 65° off-normal), and a UV−vis spectrophotometer (Lambda-900, Perkin-Elmer) was used to collect tramsmission spectra at normal incidence. A computer software package was used for the evaluation of film thickness and refractive index dispersion $n(\lambda)$. The accuracy of our measurements was validated with a spin-coated 550 nm thick PMMA film, whose refractive index profile in the 300−900 nm spectral range was found to agree with refractometric data[37] to within 0.003. The PL quantum yield was measured using the spectrofluorimeter described above with emission detected at 60° off-normal to prevent excitation light from entering the detector. The result for the anthracene-containing PMMA film, $\Phi_{PL} = 0.28 \pm 0.03$, agrees with the reported value of 0.27 in benzene and ethanol,[38] thus validating the experimental procedure. In general, the presently reported $\Phi_{PL}$ values are accompanied by an uncertainty of ±10%.

**Acknowledgment.** The authors wish to thank S. D. Jacobs and K. L. Marshall of the Laboratory for Laser Energetics, University of Rochester, for technical advice and helpful discussions. They also thank T. H. Mourey of Eastman Kodak Company for the determination of the absolute molecular weight of a polyfluorene sample. The authors are grateful for the financial support provided by the Multidisciplinary University Research Initiative, administered by the Army Research Office, under DAAD19-01-1-0676, the Defense University Research Instrumentation Program under DAAD19-00-1-0074, and the National Science Foundation under Grant CTS-9818234. Additional funding was provided by the Department of Energy Office of Inertial Confinement Fusion under Cooperative Agreement No. DE-FC03-92SF19460 with the Laboratory for Laser Energetics and the New York State Energy Research and Development Authority. The support of DOE does not constitute an endorsement by DOE of the views expressed in this article.

**Supporting Information Available:** $^1$H- and $^{13}$C-NMR spectra of **8a**, $^1$H-NMR spectra of **9a** and **10**, representative electron diffraction pattern of neat films of all five spiro-oligo(fluorene)s before and after thermal treatment, refractive index dispersion of all five compounds, absorption and PL spectra of films of **8a**, **9a**, and **10** before and after thermal annealing in air (PDF). This material is available free of charge via the Internet at http://pubs.acs.org.

CM010679L

(35) Melhuish, W. H. *J. Opt. Soc. Am.* **1964**, *54*, 183.
(36) Demas, J. N.; Crosby, G. A. *J. Phys. Chem.* **1971**, *75*, 991.
(37) Nikolov, I. D.; Ivanov, C. D. *Appl. Opt.* **2000**, *39*, 2067.
(38) Dawson, W. R.; Windsor, M. W. *J. Phys. Chem.* **1968**, *72*, 3251.